European Journal of Radiology Open 7 (2020) 100253

Contents lists available at ScienceDirect

European Journal of Radiology Open

journal homepage: www.elsevier.com/locate/ejro

Measurement of coronary artery calcium volume using ultra-high-resolution computed tomography: A preliminary phantom and cadaver study

Wataru Fukumoto [a,*], Mami Nagaoka [b,1], Toru Higaki [a,2], Fuminari Tatsugami [a,2], Yuko Nakamura [a,2], Luuk Oostveen [c,3], Willemijn Klein [c,3], Mathias Prokop [c,3], Kazuo Awai [a,2]

[a] Department of Diagnostic Radiology, Institute of Biomedical Health Sciences, Hiroshima University, Japan
[b] School of Medicine, Hiroshima University, Japan
[c] Department of Radiology and Nuclear Medicine, Radboud University Medical Center, the Netherlands

ARTICLE INFO

Keywords:
Coronary artery calcium scores
Ultra-high-resolution CT
Cadaver

ABSTRACT

Objectives: In this phantom- and cadaver study we investigated the differences of coronary artery calcium (CAC) volume on ultra-high-resolution computed tomography (U-HRCT) scans and conventional CT.

Methods: We scanned a coronary calcium phantom and the coronary arteries of five cadavers using U-HRCT in normal- and super-high resolution (NR, SHR) mode. The NR mode was similar to conventional CT; 896 detector channels, a matrix size of 512, and a slice thickness of 0.5 mm were applied. In SHR mode, we used 1792 detector channels, a matrix size of 1024, and a slice thickness of 0.25 mm. The CAC volume on NR- and SHR images were recorded. Differences in the physical- and the calculated CAC volume were defined as the error value and compared between NR- and SHR images of the phantom. Differences between the CAC volume on NR- and SHR scans of the cadavers were also recorded.

Results: The mean error value was lower on SHR- than NR images of the phantom (14.0 %, SD 11.1 vs 20.1 %, SD 15.2, $p = 0.01$). The mean CAC volume was significantly higher on SHR- than NR images of the cadavers (153.4 mm^3, SD 161.0 vs 144.7 mm^3, SD 164.8, $p < 0.01$).

Conclusions: As small calcifications were more clearly visualized on U-HRCT images in SHR mode than on conventional (NR) CT scans, SHR imaging may facilitate the accurate quantification of the CAC.

1. Introduction

Coronary artery calcium (CAC) scoring using multi-detector computed tomography (CT) is used to predict the risk for cardiovascular events including myocardial infarction and sudden cardiac death [1–3]. The CAC score correlates histologically with atherosclerotic plaque formation and it also reflects the total coronary plaque burden [2,4,5]. The CAC score is a highly specific marker for arteriosclerosis and integrates all risk factors over the lifetime of an individual [2,6,7].

The absence of CAC has been reported to reflect a very low risk for coronary mortality and morbidity, particularly in asymptomatic individuals [2,8,9]. However, possibly due to the limited spatial resolution on CT scans, in some patients, a zero CAC score does not eliminate the possibility of coronary artery disease [1,9–11]. As conventional scans for

Abbreviations: CAC, coronary artery calcium; U-HRCT, ultra-high-resolution CT; NR, normal resolution; SHR, super-high resolution; HA, hydroxyapatite; FOV, field of view; FWHM, full-width at half maximum; HU, hounsfield units; ERD, edge rise distance; ERS, edge rise slope; SD, standard deviation; ROI, region of interest; AEC, automatic exposure control; LAD, left anterior descending; LCX, left circumflex; RCA, right coronary artery; CTDI, CT dose index; DLP, dose-length product.

* Corresponding author at: Department of Diagnostic Radiology, Institute of Biomedical Health Sciences, Hiroshima University, 1-2-3 Kasumi, Minamiku, Hiroshima 734-8551, Japan.

E-mail addresses: wfukumoto@hiroshima-u.ac.jp (W. Fukumoto), b161348@hiroshima-u.ac.jp (M. Nagaoka), higaki@hiroshima-u.ac.jp (T. Higaki), fuminari@hiroshima-u.ac.jp (F. Tatsugami), yukon@hiroshima-u.ac.jp (Y. Nakamura), Oostveen@radboudumc.nl (L. Oostveen), Willemijn.Klein@radboudumc.nl (W. Klein), mathias.prokop@radboudumc.nl (M. Prokop), awai@hiroshima-u.ac.jp (K. Awai).

[1] School of Medicine, Hiroshima University, 1-2-3 Kasumi, Minamiku, Hiroshima 734-8551, Japan.
[2] Department of Diagnostic Radiology, Institute of Biomedical Health Sciences, Hiroshima University, 1-2-3 Kasumi, Minamiku, Hiroshima 734-8551, Japan.
[3] Department of Radiology and Nuclear Medicine, Radboud University Medical Center, Radboud University, Houtlaan 4, 6525 XZ, Nijmegen, the Netherlands.

https://doi.org/10.1016/j.ejro.2020.100253
Received 30 July 2020; Accepted 24 August 2020
Available online 8 September 2020

the acquisition of CAC scores tend to use 2.5–3.0-mm-thick slices, partial volume effects may result in missing small calcifications [1]. According to Urabe et al. [9], on 0.5-mm slices, small calcifications were detectable and useful for predicting coronary plaques and coronary stenosis in patients with zero CAC scores on conventional 3.0-mm slice reconstructions.

Ultra-high-resolution CT (U-HRCT) with 0.25-mm collimation and a 1024 matrix is now used in clinical studies [5,12–20]. As the spatial resolution of U-HRCT is 150 μm and thus higher than of conventional CT, it may facilitate the detection of small coronary calcifications and the accurate quantification of the CAC.

We investigated the differences of CAC volume on normal- and super-high resolution (NR, SHR) U-HRCT images of a phantom and of five human cadavers.

2. Materials and methods

2.1. Phantom study

We scanned a coronary calcium calibration phantom (QRM-Cardio-Phantom: QRM GmbH, Moehrendorf, Germany) on a U-HRCT scanner (Aquilion Precision; Canon Medical Systems, Japan) that features a normal-, a high-, and a super-high scan mode (NR, HR, SHR). The NR mode is similar to the mode used for conventional CT studies; 896 detector channels are used and a 512 × 512 matrix size and a 0.5-mm slice thickness are available. In HR mode, 1792 detector channels are used, 512 × 512-, 1024 × 1024-, and 2048 × 2048 matrix sizes and a 0.5-mm slice thickness are available. In SHR mode, a slice thickness of 0.25 mm is available; the other parameters are as in HR mode [14]. We applied the NR- and the SHR mode for scanning the phantom.

As shown in Fig. 1, the phantom was 200 × 300 mm in its body diameter, the depth was 100 mm. It featured a spine insert surrounded by soft tissue-equivalent material and an artificial lung. Compartments

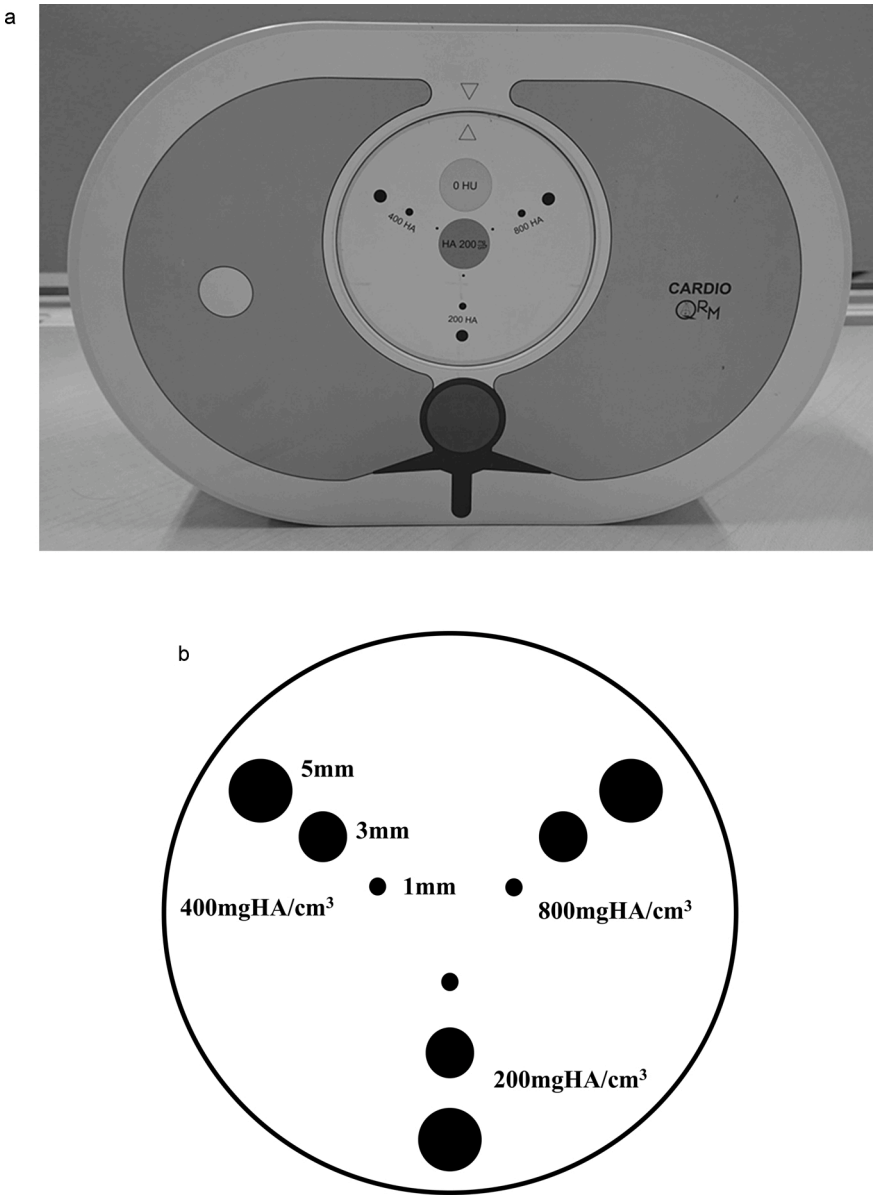

Fig. 1. Our coronary calcium calibration phantom.
(a) Photograph of the coronary calcium calibration phantom (body diameter: 200 × 300 mm, depth: 100 mm).
(b) The phantom harbors 1-, 3-, and 5-mm-diameter cylindrical calcifications comprised of 200-, 400-, and 800 mg hydroxyapatite (HA)/cm^3 each.

representing the heart contained cylindrical calcifications measuring 1−, 3−, and 5 mm in diameter, they were comprised of 200−, 400−, and 800 mg hydroxyapatite (HA)/cm^3. The physical volume of the 1−, 3−, and 5-mm calcifications which were recorded in the instruction were 0.8−, 21.2−, and 98.2 mm^3, respectively.

Volume scans were performed at 80 × 0.5 mm and with 896 channels (NR mode) and at 160 × 0.25 mm with 1792 channels (SHR mode). We acquired five scans in each mode. The focus size was 0.6 × 1.3 mm (NR mode) and 0.4 × 0.5 mm (SHR mode). As in an earlier study [21], the reference standard exposure settings were tube voltage 120 kVp, tube current 250 mA. In NR- and SHR mode the rotation time was 0.35 s, the field of view (FOV) was 250 mm. The reconstruction algorithm was model-based reconstruction (Forward projected model-based Iterative Reconstruction SoluTion Body standard; Canon Medical Systems, Japan). In NR mode the matrix size was 512 × 512, the slice thickness was 0.5 mm; in SHR mode, they were 1024 × 1024 and 0.25 mm.

The CAC volume were calculated as: number of voxels over the threshold CT value x volume of one voxel. The threshold CT value was determined as: [(maximum CT value of the calcification) + (CT value of the soft tissue-equivalent material)] / 2. We applied the full-width at half maximum (FWHM) method [22–24]; it is commonly used for quantitative measurements on CT images to increase the accuracy of quantitative data. When the threshold CT value was less than 130 Hounsfield units (HU) we adopted 130 HU, i.e. the threshold applied in clinical settings [25]. The error value (%) was defined as: {[(calculated volume) – (physical volume)] / (physical volume)} x 100. We compared the mean error value of nine calcifications scanned in NR- and SHR mode.

Two board-certified radiologists with 11 and 17 years of experience with CT image interpretation evaluated the visibility of cylindrical calcifications.

Using Image J software (NIH, Bethesda, MD) and its particle analysis tool (Plot profile) we generated a profile curve for each calcification scanned in NR- and SHR mode to compare the effect of blooming artifacts. As shown in Fig. 2, we measured the width of the edge response of the calcifications, determined by the 10–90 % edge rise distance (ERD), and calculated the edge rise slope (ERS) as: ERS = (CT90 %-CT10 %)/ERD [26]. The ERD and ERS were examined on both sides and the ERS obtained in NR- and SHR mode was compared.

The image noise, determined as the standard deviation (SD) of the attenuation value in a single circular region of interest (ROI, about 100 mm^2) placed in the homogeneous soft tissue-equivalent material was measured on axial NR- and SHR images.

2.2. Cadaver study

We used five human cadavers. Ethical approval was waived as the individuals had provided written consent for their use in scientific procedures. Their permission is also in accordance with Dutch law. Demographic data on the cadavers are shown in Table 1.

The coronary arteries were scanned twice on a U-HRCT scanner in NR- and SHR mode. Volume scans were performed at a tube voltage of 120 kVp, the tube current was regulated by automatic exposure control (AEC). The preset noise value was 40 HU, the slice thickness was 0.5 mm. Other parameters were: rotation time 0.35 msec, beam collimation 896 channels, 0.5 mm x 80 rows (NR mode); in SHR mode they were 1792 channels, 0.25 mm x 160 rows. The focus size was automatically selected depending on the scan conditions (Table 1). In NR mode the image matrix was 512 × 512, the slice thickness was 0.5 mm, in SHR mode they were 1024 × 1024 and 0.25 mm. The FOV was 250 mm.

We recorded the CAC volume of the left anterior descending-, the left circumflex-, and the right coronary artery (LAD, LCX, RCA) on images reconstructed with model-based iterative reconstruction using a commercially-available image processing workstation (Virtual Place Plus; Aze, Tokyo, Japan). The CAC volume is the summed volume of all voxels within coronary arteries whose HU exceeded 130 HU.

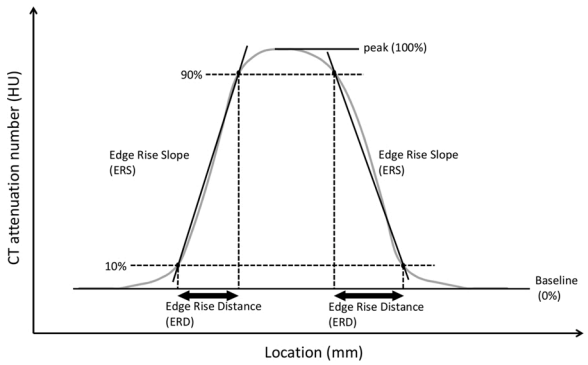

Fig. 2. Phantom study. Profile curve of calcifications. To assess blooming artifacts, we measured the width of the edge response. The edge rise distance (ERD) and the edge rise slope (ERS) at a pixel attenuation ranging from 10 to 90 % of the maximum CT attenuation are shown.

The difference (%) in the CAC volume obtained in NR- and SHR mode was defined as: {[(SHR volume) – (NR volume)] / NR volume} x 100. To assess the relationship between the difference value and the CAC volume obtained in NR mode we performed simple regression analysis.

The image noise, determined as the SD of the attenuation value in a single circular 100-mm^2 ROI placed in the ascending aorta was measured on axial NR- and SHR images.

The calculated volume CT dose index ($CTDI_{vol}$) and the dose-length product (DLP) were recorded as the radiation dose. The effective dose was calculated using a standard conversion factor of 0.014 mSv/mGy for chest CT studies.

Statistical differences were determined with the two-sided paired *t*-test. Differences of $p < 0.05$ were considered statistically significant. We use software for statistical analysis (JMP software, SAS Institute, Cary, NC).

3. Results

3.1. Phantom study

The mean volume and error value of 1−, 3−, and 5 mm diameter calcifications comprised of 200−, 400−, and 800 mg HA cm^3, respectively, are presented in Table 2. In NR mode, the mean error value was 20.1 % (SD 15.2); in SHR mode it was 14.0 % (SD 11.1). The mean error value was significantly lower on SHR- than NR images ($p = 0.01$).

On NR images, both radiologists identified all but the smallest and lowest density calcification (1-mm and 200 mg HA/cm3). On SHR images the error value of the smallest and lowest density calcification was high (43.3 %), all calcifications were clearly detectable. Representative images are shown in Fig. 3.

The mean ERS for calcifications on NR- and SHR images were 404.0 (SD 296.6) and 558.2 (SD 332.4) HU/mm, respectively. The mean ERS on SHR images were significantly higher than on NR images ($p < 0.01$).

The image noise was higher on SHR- than NR images [25.0− (SD 0.06) vs 18.2 (SD 0.03)].

3.2. Cadaver study

The mean CAC volume for the LAD, LCX, and RCA in the five cadavers was 153.4 (161.0) mm^3 in SHR- and 144.7 (164.8) mm^3 in NR mode. The relationship between the difference value and the CAC volume obtained in NR mode is shown in Fig. 4. Simple regression analysis revealed a negative correlation between the difference value and the CAC volume on NR images although the correlation coefficient was not strong ($R = 0.55$, $p = 0.03$).

The mean $CTDI_{vol}$ and DLP were 7.4 (SD 4.0) mGy and 137.7 (SD

Table 1
Basic data on five cadavers.

Cadaver number	Gender	Age (years old)	Height (cm)	Weight (kg)	BMI (kg/m^2)	Postmortem interval	Cause of death	Focus size (mm) NR	Focus size (mm) SHR
1	Male	83	165	51	18.7	5h30	Parkinson and dementia	0.4 × 0.5	0.4 × 0.5
2	Male	61	170	84	29.1	26h40	Lung cancer	0.6 × 1.3	0.6 × 1.3
3	Male	86	160	60	23.4	6h15	Lung cancer	0.4 × 0.5	0.4 × 0.5
4	Female	70	162	81	30.9	5h30	Colon cancer meta	0.6 × 1.3	0.6 × 1.3
5	Female	97	162	62	23.6	18h	Natural senile decay	0.6 × 0.6	0.6 × 1.3

BMI: body mass index.
NR: normal resolution.
SHR: super high resolution.

Table 2
Phantom study: Mean volume and error value of calcifications.

Calcification		Mean volume (mm^3)		Error value (%)	
Density (mg HA/cm^3)	Size (mm)	NR	SHR	NR	SHR
800	5	93.7	93.2	4.6	5.1
	3	17.3	18.8	18.5	11.3
	1	1.1	0.8	40.1	2.8
400	5	89.7	89.6	8.6	8.7
	3	17.9	18.8	15.5	11.5
	1	1.2	0.9	49.0	15.5
200	5	92.8	85.0	5.5	13.4
	3	17.1	18.2	19.1	14.3
	1	ND	1.1	ND	43.4
Mean				20.1	14.0
Standard deviation				15.2	11.1

HA: hydroxyapatite.
NR: normal resolution.
SHR: super high resolution.
ND: not detectable.

79.6) mGycm in NR mode. They were 16.1 (SD 8.0) mGy and 298.4 (SD 153.1) mGycm in SHR mode (both $p = 0.02$). The mean effective dose was 1.9 mSv in NR- and 4.2 mSv in SHR mode. The mean image noise was 23.2 HU (SD 3.0) in NR- and 34.5 HU (SD 5.5) in SHR mode ($p < 0.01$). The radiation dose and the image noise were significantly higher on SHR- than NR images.

4. Discussion

Our evaluation of the CAC volume on U-HRCT images of a phantom and of five human cadavers showed that on phantom scans, small calcifications were more accurately detectable on SHR- than NR images. In the cadaver study, the mean volume score of the coronary arteries was significantly higher on SHR- than NR scans, probably because the spatial resolution is higher on SHR- than NR-, i.e. conventional CT images. Representative images are shown in Fig. 5.

Because in humans the coronary artery can harbor different amounts and forms of calcifications and their distribution is more complex than in our phantom, we compared the results of the phantom- and cadaver studies. On cadaver scans there was a negative correlation between the differences value and the amount of CAC volume; the difference in the CAC volume of NR- and SHR images was larger for arteries with a low CAC volume. The profile curve of phantom images showed that on U-HRCT scans acquired in SHR mode, blooming artifacts were reduced; consequently, the CAC volume was lower [21]. This effect may compensate the increase of CAC volume by detecting small calcifications, particularly among the coronary arteries with high CAC volume. In the other words, U-HRCT with SHR mode may not influence the outcome clinically in patients with high degrees of coronary artery calcification. Thus, the measuring the CAC using U-HRCT may allow for a more precise risk classification in patients with low degrees of coronary artery calcification.

Although a zero calcium score is associated with a low risk for cardiovascular events [2,8,9], other studies [1,9–11] showed that it does not eliminate the presence of obstructive disease. In the CoRE-64 study [27], 19 % of patients with a zero CAC score manifested obstructive disease. According to Urabe et al. [9], in patients with a zero CAC score,

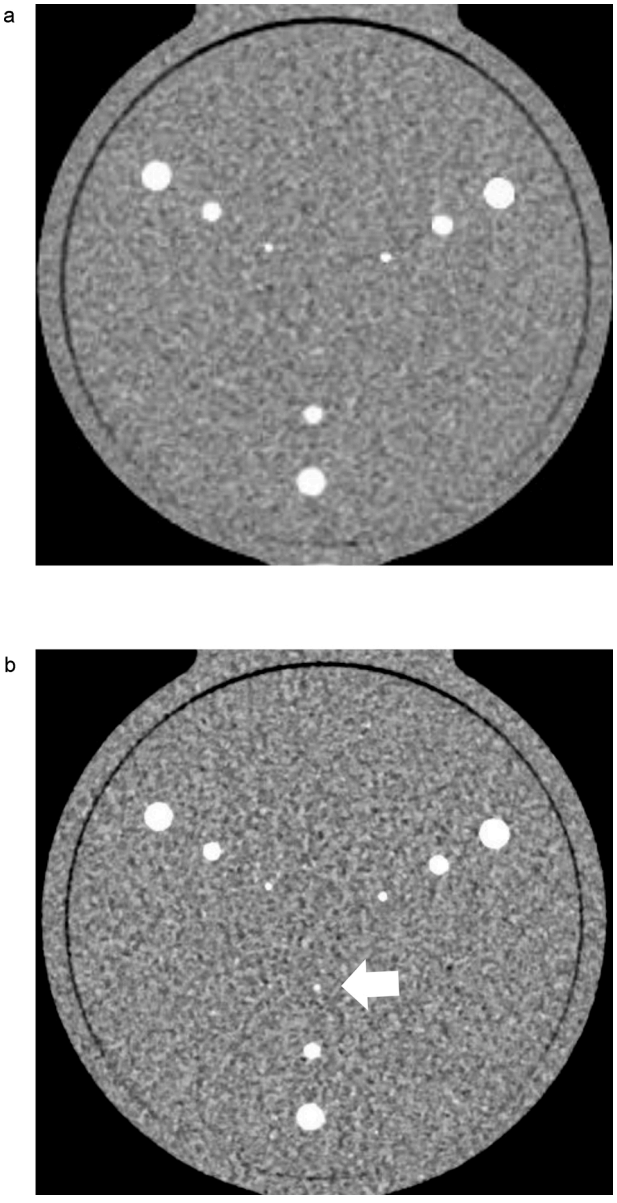

Fig. 3. Phantom study. CT scans were obtained in (a) NR- and in (b) SHR mode. The smallest and lowest density calcifications (1-mm and 200 mg HA/cm3) were clearly identifiable only in SHR mode (arrow).

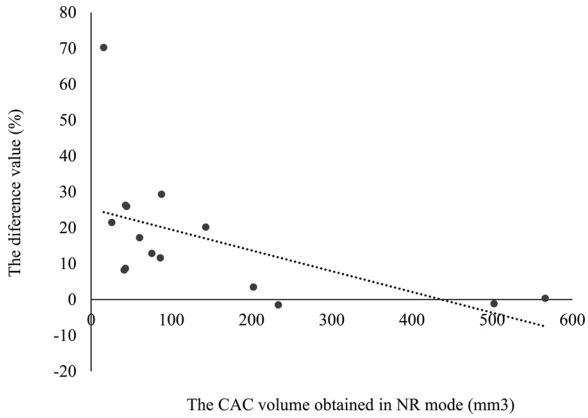

Fig. 4. Plot of the difference value and the CAC volume obtained in NR mode. Simple regression analysis revealed a negative correlation between the difference value and the CAC volume.

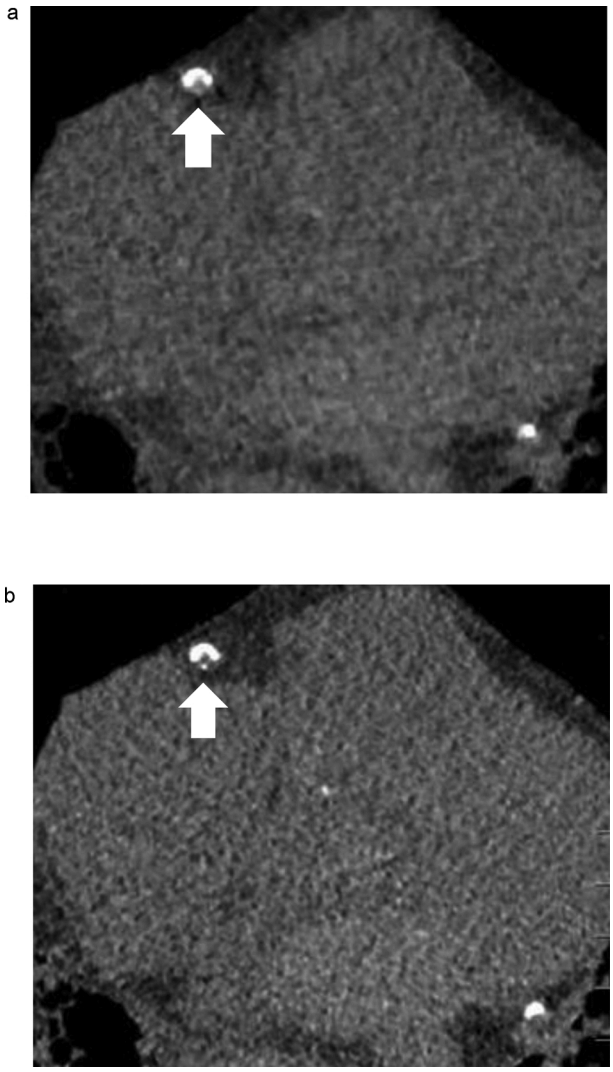

Fig. 5. CT images of the right coronary artery in an 83-year-old male corpse. The scans were obtained in (a) NR- and (b) in SHR mode. On the scan obtained in SHR mode, small spotty calcifications are clearly identified (arrows).

0.5-mm slices were superior to 3-mm slices for the detection of small calcifications and thus for assessing the risk for obstructive and non-obstructive coronary artery disease. They also reported that patients with small calcifications presented with more coronary risk factors than did patients without such calcifications. Therefore, the detection of small CACs is important for assessing the risk for cardiovascular events in patients with a zero CAC score on conventional CT scans.

The mean error value of calcifications using U-HRCT with SHR mode was 14.0 % and it was superior value compared to previous studies [5,28,29]. The error is mainly attributable to voxels in tissues adjacent to calcified structures. Due to the partial volume effect, their attenuation might result in values that exceed the calcium scoring threshold and be included in the volume score [29]. As the partial volume effect is reduced on 0.25-mm slices acquired in SHR mode, the volume score may be close to the true value. In earlier investigations the interscan variability among volume scores ranged from 9 to 16 % [5,25], therefore, we consider the CAC volume we calculated to be acceptable in clinical settings.

CAC volume was used instead of CAC scores in this study because it is simply calculated as the product of the number of voxels containing calcium and the volume of one voxel [25,30]. This allows for linear augmentation in the CAC volume as calcium increases. The physical volume of calcifications was also known in the phantom study. Although the Agatston score which is calculated by multiplying the weighting factor by the area of calcification is widely used in clinical settings, it does not correspond to a physical measure, so it cannot be easily compared to a true value. Also, the Agatston score increase nonlinearly with increases in the amount of CAC [25]. Therefore, measurement of CAC volume is adequate for the investigating the difference of CAC on U-HRCT which has higher spatial resolution.

Due to relatively insufficient incident photons on smaller detectors, the radiation dose and image noise present problems when CAC is evaluated on U-HRCT images [12]. We found that the radiation dose and image noise were significantly higher on SHR- than NR images; the increased image noise rendered reliable discrimination between small calcifications and image noise difficult. A reduction in the image noise requires higher radiation exposure at U-HRCT. The Society of Cardiovascular Computed Tomography (SCCT) recommends radiation doses of 1.0− to 1.5 mSv for image acquisition. The effective dose for the acquisition of SHR images in our cadaver study was about 4.0 mSv, thus exceeding the clinically-allowable dose. The new CT image reconstruction methods that involve deep convolutional neural networks improve the image quality and reduce the image noise and may help to resolve the problems encountered with U-HRCT [12,31].

Our study has some limitations. Our phantom was motion-free and the cadaver study did not account for the effect of cardiac motion. However, we thought evaluating the CAC measurements on U-HRCT in ideal conditions was important as a preliminary study. Also, to increase the accuracy of our quantitative data, we calculated the CAC volume in our phantom study by applying the FWHM method. The maximum density of each coronary calcification should be assessed although such determinations are not feasible in clinical settings. Therefore, we used 130 HU as the threshold in our cadaver study.

Based on our findings we conclude that U-HRCT in SHR mode is superior to scans obtained in NR mode for the detection of small coronary calcifications. It may facilitate the accurate assessment of the CAC.

Funding

This research did not receive any specific grant from funding agencies in the public, commercial, or not-for-profit sectors.

CRediT authorship contribution statement

Wataru Fukumoto: Conceptualization, Methodology, Validation, Writing - original draft. **Mami Nagaoka:** Investigation, Data curation. **Toru Higaki:** Data curation. **Fuminari Tatsugami:** Supervision. **Yuko Nakamura:** Supervision. **Luuk Oostveen:** Data curation. **Willemijn**

Klein: Investigation. **Mathias Prokop:** Supervision, Project administration. **Kazuo Awai:** Supervision, Project administration.

Declaration of Competing Interest

The co-authors (Mathias Prokop, Kazuo Awai) of this manuscript declare relationships with the following companies: Canon Medical Systems Co. Ltd.

References

[1] N. van der Bijl, P.W. de Bruin, J. Geleijns, et al., Assessment of coronary artery calcium by using volumetric 320-row multi-detector computed tomography: comparison of 0.5 mm with 3.0 mm slice reconstructions, Int. J. Cardiovasc. Imaging 26 (2010) 473–482.

[2] N. Malguria, S. Zimmerman, E.K. Fishman, Coronary artery calcium scoring: current Status and review of literature, J. Comput. Assist. Tomogr. 42 (2018) 887–897.

[3] P.C. Keelan, L.F. Bielak, K. Ashai, et al., Long-term prognostic value of coronary calcification detected by electron-beam computed tomography in patients undergoing coronary angiography, Circulation 104 (2001) 412–417.

[4] J.A. Rumberger, D.B. Simons, L.A. Fitzpatrick, et al., Coronary artery calcium area by electron-beam computed tomography and coronary atherosclerotic plaque area. A histopathologic correlative study, Circulation 92 (1995) 2157–2162.

[5] C. Hong, K.T. Bae, T.K. Pilgram, Coronary artery calcium: accuracy and reproducibility of measurements with multi-detector row CT–assessment of effects of different thresholds and quantification methods, Radiology 227 (2003) 795–801.

[6] A. Rozanski, D.S. Berman, Coronary artery calcium scanning in symptomatic patients: ready for use as a gatekeeper for further testing? J. Nucl. Cardiol. 24 (2017) 835–838.

[7] R. Erbel, M. Budoff, Improvement of cardiovascular risk prediction using coronary imaging: subclinical atherosclerosis: the memory of lifetime risk factor exposure, Eur. Heart J. 33 (2012) 1201–1213.

[8] M.J. Budoff, R.L. McClelland, K. Nasir, et al., Cardiovascular events with absent or minimal coronary calcification: the multi-ethnic study of atherosclerosis (MESA), Am. Heart J. 158 (2009) 554–561.

[9] Y. Urabe, H. Yamamoto, T. Kitagawa, et al., Identifying small coronary calcification in Non-contrast 0.5-mm slice reconstruction to diagnose coronary artery disease in patients with a conventional zero coronary artery calcium score, J. Atheroscler Thromb. 23 (2016) 1324–1333.

[10] I. Gottlieb, J.M. Miller, A. Arbab-Zadeh, et al., The absence of coronary calcification does not exclude obstructive coronary artery disease or the need for revascularization in patients referred for conventional coronary angiography, J. Am. Coll Cardiol. 55 (2010) 627–634.

[11] H. Yamamoto, N. Ohashi, K. Ishibashi, et al., Coronary calcium score as a predictor for coronary artery disease and cardiac events in Japanese high-risk patients, Circ J. 75 (2011) 2424–2431.

[12] M. Akagi, Y. Nakamura, T. Higaki, et al., Deep learning reconstruction improves image quality of abdominal ultra-high-resolution CT, Eur. Radiol. (2019), https://doi.org/10.1007/s00330-019-06170-06173.

[13] H. Takagi, R. Tanaka, K. Nagata, et al., Diagnostic performance of coronary CT angiography with ultra-high-resolution CT: comparison with invasive coronary angiography, Eur. J. Radiol. 101 (2018) 30–37.

[14] A. Hata, M. Yanagawa, O. Honda, et al., Effect of matrix size on the image quality of ultra-high-resolution CT of the lung: comparison of 512 x 512, 1024 x 1024, and 2048 x 2048, Acad. Radiol. (25) (2018) 869–876.

[15] O. Honda, M. Yanagawa, A. Hata, et al., Influence of gantry rotation time and scan mode on image quality in ultra-high-resolution CT system, Eur. J. Radiol. 103 (2018) 71–75.

[16] N. Tanabe, T. Oguma, S. Sato, et al., Quantitative measurement of airway dimensions using ultra-high resolution computed tomography, Respir Investig. 56 (2018) 489–496.

[17] M. Yanagawa, A. Hata, O. Honda, et al., Subjective and objective comparisons of image quality between ultra-high-resolution CT and conventional area detector CT in phantoms and cadaveric human lungs, Eur. Radiol. 28 (2018) 5060–5068.

[18] S. Motoyama, H. Ito, M. Sarai, et al., Ultra-High-Resolution computed tomography angiography for assessment of coronary artery stenosis, Circ. J. 82 (2018) 1844–1851.

[19] K. Yoshioka, R. Tanaka, H. Takagi, et al., Ultra-high-resolution CT angiography of the artery of adamkiewicz: a feasibility study, Neuroradiology 60 (2018) 109–115.

[20] K. Yamashita, A. Hiwatashi, O. Togao, et al., Ultrahigh-resolution CT scan of the temporal bone, Eur. Arch. Otorhinolaryngol. 275 (2018) 2797–2803.

[21] S. Oda, D. Utsunomiya, T. Nakaura, et al., The influence of iterative reconstruction on coronary artery calcium scoring-phantom and clinical studies, Acad. Radiol. 24 (2017) 295–301.

[22] R. Dautry, M. Edjlali, P. Roca, et al., Interest of HYPR flow dynamic MRA for characterization of cerebral arteriovenous malformations: comparison with TRICKS MRA and catheter DSA, Eur. Radiol. 25 (2015) 3230–3237.

[23] S. Achenbach, S. Ulzheimer, U. Baum, et al., Noninvasive coronary angiography by retrospectively ECG-gated multislice spiral CT, Circulation 102 (2000) 2823–2828.

[24] A. Ikemura, I. Yuki, H. Suzuki, et al., Time-resolved magnetic resonance angiography (TR-MRA) for the evaluation of post coiling aneurysms; A quantitative analysis of the residual aneurysm using full-width at half-maximum (FWHM) value, PLoS One 13 (2018), e0203615.

[25] K. Alluri, P.H. Joshi, T.S. Henry, et al., Scoring of coronary artery calcium scans: history, assumptions, current limitations, and future directions, Atherosclerosis 239 (2015) 109–117.

[26] F. Tatsugami, T. Higaki, H. Sakane, et al., coronary artery stent evaluation with model-based iterative reconstruction at coronary CT angiography, Acad Radiol. 24 (2017) 975–981.

[27] A. Sarwar, L.J. Shaw, M.D. Shapiro, et al., Diagnostic and prognostic value of absence of coronary artery calcification, JACC Cardiovasc Imaging 2 (2009) 675–688.

[28] P.H. Tseng, S. Mao, D.Z. Chow, et al., Accuracy in quantification of coronary calcification with CT: a cork-dog heart phantom study, Acad Radiol. 17 (2010) 1249–1253.

[29] C.K. Thomas, G. Muhlenbruch, J.E. Wildberger, et al., Coronary artery calcium scoring with multislice computed tomography: in vitro assessment of a low tube voltage protocol, Invest. Radiol. 41 (2006) 668–673.

[30] T.Q. Callister, B. Cooil, S.P. Raya, et al., Coronary artery disease: improved reproducibility of calcium scoring with an electron-beam CT volumetric method, Radiology 208 (1998) 807–814.

[31] F. Tatsugami, T. Higaki, Y. Nakamura, et al., Deep learning-based image restoration algorithm for coronary CT angiography, Eur Radiol. (2019), https://doi.org/10.1007/s00330-019-06183-y.